INTERNATIONAL JOURNAL OF CIVIL ENGINEERING AND TECHNOLOGY (IJCIET)

ISSN 0976 – 6308 (Print)
ISSN 0976 – 6316(Online)
Volume 4, Issue 2, March - April (2013), pp. 58-79
© IAEME: www.iaeme.com/ijciet.asp
Journal Impact Factor (2013): 5.3277 (Calculated by GISI)
www.jifactor.com

IJCIET
© IAEME

SEISMIC CHARACTERISTICS OF THE FOLDED CANTILEVER SHEAR STRUCTURE

Ercan Serif Kaya[a], Takuro Katayama[b] and Toshitaka Yamao[c]

[a] Architectural and Civil Engineering, GSST, Kumamoto University, 860-8555, Kumamoto
[b] Faculty of Engineering, Eco Design, Sojo University, 860-0082, Kumamoto, Japan
[c]Architectural and Civil Engineering, GSST, Kumamoto University, 860-8555, Kumamoto, Japan

ABSTRACT

A newly designed structure named folded cantilever shear structure (FCSS) is proposed as an alternative seismic isolation approach that combines coupling method and roller bearings in one structure for improving earthquake resistant ability and seismic performance of mid-rise buildings. Seismic characteristics of the proposed structure have been investigated by conducting numerical analyses on the idealized vibration model with and without additional viscous dampers. Dynamic parameters such as natural frequencies, damping ratios and mode shapes, and seismic responses due to elastic dynamic response analysis were also obtained under four exemplary ground motions, namely El-Centro, Hachinohe, Miyagi and Taft earthquakes. The proposed structure consists of fix-supported shear sub-frame and movable shear sub-frame supported by roller bearings, and these fully-separated sub-frames were rigidly connected by a connection sub-frame at the top point. This will allow all three sub-frames to behave as a unique structure to increase the overall seismic performance. It was found that the proposed structure is capable of extending natural period and minimizing accelerations, displacements and base shear forces simultaneously, when compared to ordinary structure which has the same number of storey. However, relative displacements, for the proposed structure without additional dampers, with respect to the base were obtained relatively higher. Therefore, additional viscous dampers were added between adjacent beams to connect both sub-frames with the aim of avoiding excessive displacements and increasing the damping ratio as well.

Keywords: seismic performance; mid-rise building; additional viscous damper; natural period; roller bearing; coupling.

1. INTRODUCTION

Base isolation systems have become one of the most widely used and well-adopted seismic isolation measures providing numerous alternatives to design optimum solution for the structures in reducing seismic responses. What makes base isolation systems more attractive is that these isolation systems are increasingly implemented and tested in practice result in satisfying seismic performance. Moreover, base isolation systems, contrary to strengthening methods which are common measures for seismic isolation, can simultaneously reduce floor accelerations and relative displacement of floors with respect to base [1], and can be implemented for any height of structure that already exist or newly designed.

Another seismic isolation method which has mainly applied to mid-rise buildings and increasingly become an interest of area is coupling method enabling connection of adjacent structures using rigid elements or passive damper devices in reducing seismic responses. Coupling method is similar to base isolation method in that it also can be implemented either in existing or newly designed structures not only for reducing pounding possibility but also increasing seismic performance. Ohami *et al*., tried to improve the seismic reliability of an existing structure built in accordance with old provisions of building codes of Japan before revisions were made in 1981. Different heights of buildings, one is 5-storey representing old building and the other is 10-storey building representing newly designed building, were selected to be idealized shear models for numerical analysis and interconnections were made by using rigid connection elements and viscous dampers. The reason for choosing buildings of different heights was reported that responses of coupled buildings could not be reduced when similar height of buildings was chosen [2]. However, it should be noted that researchers mainly used coupling method on buildings of fixed boundary conditions. As a result, it was found that it is more effective to design new building to be connected to old one as stiff building instead of flexible building with rigid connection elements, and rigid connection elements were insufficient to prevent the collapse of 5-storey old building when incorporated in flexible building. Another notable study was carried out [3] using experimental building models coupling 12-storey building model to 3-storey low-rise podium structure in 3 different configurations which are respectively fully-separated, rigidly connected and friction damped-linked. According to the results, passively controlled buildings provided most effective performance when compared to other cases. Interestingly, the rigidly connected buildings gave rise to increase in seismic responses. Xu *et al*. also stated that fluid damper connected buildings are more effective in reducing seismic responses for lower adjacent buildings than of higher ones and fluid dampers are more favorable for buildings of same height than those of different heights [4].

Aida *et al*., tried to improve the damping performance of adjacent structures by linking them using only one member which consists of only one spring and one damper element that was a soft member. It was found that the damping performance increases as long as first natural periods of structures become different and the most effective connection part for the structures was obtained near to the top part of the structures [5].

As above mentioned, Agarwal *et al*. confirmed that most of buildings have been configured with fixed conditions since base isolation is a relatively new modification technique [6]. Therefore, they studied pounding response of two friction varying base isolated

buildings to clarify the seismic behavior of adjacent buildings of similar heights. The analyses of two buildings were conducted in three cases which are single base isolated building, adjacent buildings without base isolation and base isolated buildings. According to the results, there was little or no interaction between buildings for the case of single base isolated building. In another study, Abdullah used shared tuned mass system connecting two 8-storey buildings to each other at the roof with the aim of decreasing the overall response of the buildings and pounding possibility, as well [7].

In the view of these studies, it can be summarized that coupling method can be effective solution to deal with the problem of not only pounding but also decreasing seismic responses of mid-rise buildings. However, most of researchers used buildings of different heights with fix-supported conditions. When using buildings of similar heights, fixed-supported buildings are likely to be insufficient in increasing seismic performance. Therefore, buildings of these configurations to be connected can be supported by viscous damping devices for favorable outcome. As for buildings of similar heights, it is also another option to connect them at the roof but, for the case of fixed-supported buildings, soft connection element can be more effective on overall responses if buildings are dissimilar in terms of natural frequency.

The main objective of this study is to propose an alternative seismic isolation approach incorporating base isolation system and coupling method into a mid-rise structure with the aim of increasing seismic performance and natural period. Therefore, a new configuration of buildings of similar heights has been studied by connecting them at the roof part. The boundary conditions were selected to be one fixed supported building and the other one to be base isolated building while using rigid connection element at the top part. In order to investigate seismic characteristics of the proposed vibration model, numerical analyses were conducted on the idealized vibration model with and without additional viscous dampers. As for damper-added buildings, some studies have been proposed offering practical and effective damper placement methods [8-11] and some of these placement methods were compared by Whittle in terms of effectiveness [12]. Despite of these methods' benefits, these techniques are for advanced optimization, and the vibration model of our study with additional viscous dampers was assumed to be uniformly distributed to clarify whether the newly designed structure is effective in reducing seismic responses.

A standard acceleration response spectrum of an ordinary structure with 5% damping ratio is given in Fig. 1. The natural period of an ordinary mid-rise structure is likely to be around 1 sec, and as expected, the acceleration of the structure reduces as long as period increases. As for the proposed structure named folded cantilever shear structure (FCSS), it is able to extend the first natural period almost two times compared to ordinary folded cantilever shear structure (OCSS), by increasing the floor number by a factor of two without changing the total height of structure. For this purpose, the proposed structure is designed consists of three main parts, namely, fix-supported shear sub-frame, movable shear sub-frame which is supported by roller bearings and connection sub-frame at the top part connecting these sub-frames to each other and uniting them as one structure. Besides, adjacent beams of sub-frames were connected to each other by additional viscous dampers to avoid excessive displacements and to increase the damping ratio as well.

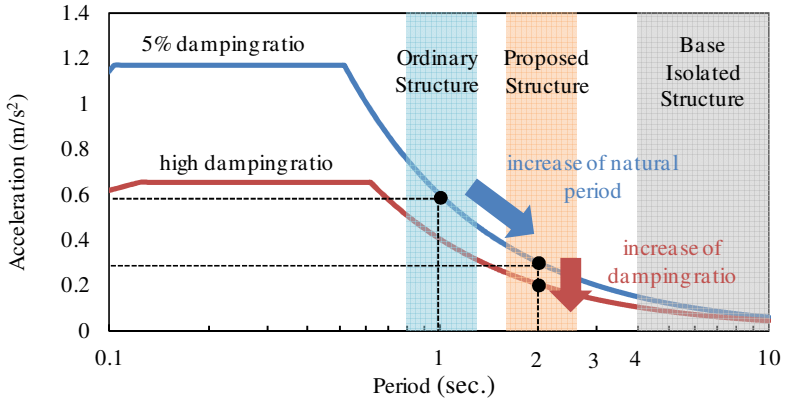

Fig. 1 Standard acceleration response spectrum due to increasing period and damping ratio

2. NATURAL VIBRATION CHARACTERISTICS OF A MULT-STOREY STRUCTURE

2.1 Vibration model

In this section, the natural vibration characteristics of an ordinary multi-storey structure are theoretically given.

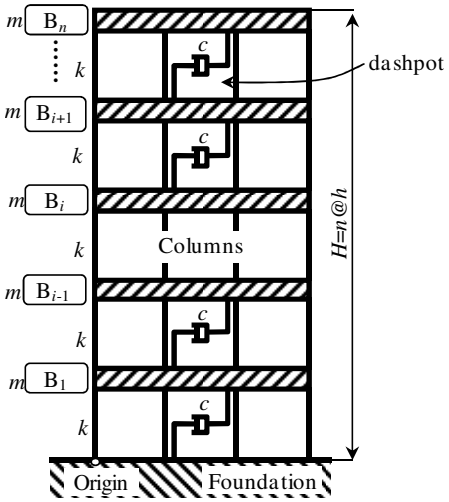

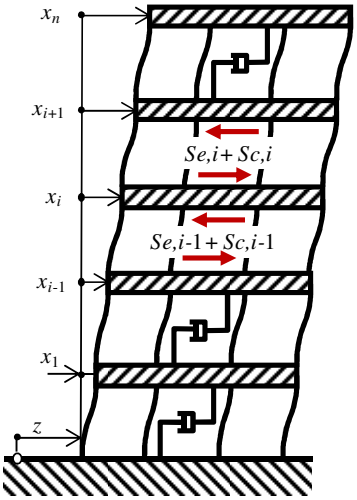

Fig. 2 Ordinary structure system-O **Fig. 3** Deformed frame of system-O

Fig. 2 illustrates a two-dimensional vibration model of an ordinary multi-storey shear structure. The vibration model, named as system-O, has fixed end consisting n number of storey. Beams are represented as B_1, B_2, ···, Bn, and columns and dashpots are identical in terms of dynamic characteristics for each storey. The letter m stands for the mass of beam, k is the shear spring coefficient of column and c is the viscous damping coefficient of dashpot to represent the structural damping of idealized vibration model. The total height of the n-storey vibration model is H and each storey has a height of h, $H=nh$. The beams are carrying the concentrated masses of beams and columns at their center.

2.2 The equation of motion of ordinary structure under base excitation

The deformed frame and the internal forces of system-O due to displacement excitation are illustrated in Fig. 3, under *z(t)* time-varying ground motion, where z is the relative displacement of the base from its origin and $x_1, x_2, \cdots, x_n$ are the lateral displacements of beam B_1, B_2, ⋯, B_n. The relative displacement for the i-th storey, B_i, is $z + x_i$ whereas shear and viscous damping forces between beam B_i and B_{i+1} are represented as $S_{e,i}$ and $S_{c,i}$, respectively. The inertia force of beam B_i is also represented as S_m. The equilibrium of the forces of beams are become as following equation,

$$-S_{m,i} + S_{c\,i} - S_{c,i\text{-}1} + S_{e,i} - S_{e,i\text{-}1} = 0,\ 1 \le i < n \tag{1}$$

$$-S_{m,n} - S_{c,n\text{-}1} - S_{e,n\text{-}1} = 0$$

The shear, viscous damping and the inertia forces between the beams can be expressed as $S_{e,i} = k\left(x_{i+1}\text{-}x_i\right)$, $S_{c,i} = c\left(\dot{x}_{i+1}\text{-}\dot{x}_i\right)$ and $S_{m,i} = m(\ddot{z}+\ddot{x}_i)$, respectively where $\dot{x}_i$ and $\ddot{x}_i$ stands for first and second derivation of displacement, x_i. And $\ddot{z}$ is the acceleration of the ground.

With respect to ground floor, shear and damping forces of the beam can be expressed as $S_{e,0} = k(x_1)$ and $S_{c,0} = c(\dot{x}_1)$, respectively. After substituting these equations of the forces into Eq. (1), the equation of the motion of system-O due to lateral displacement excitation becomes as the following equation,

$$M^{(n)}\ddot{x}^{(n)} + C^{(n)}\dot{x}^{(n)} + K^{(n)}x^{(n)} = -\ddot{z}M^{(n)}p^{(n)} \tag{2}$$

Where, $p^{(n)}$ is the column vector which has all its elements equal to 1, $x^{(n)} \equiv \left[x_1, x_2, \cdots, x_n\right]^{\mathrm{T}}$, $\dot{x}^{(n)} \equiv [\dot{x}_1, \dot{x}_2, \cdots, \dot{x}_n]^{\mathrm{T}}$ and $\ddot{x}^{(n)} \equiv [\ddot{x}_1, \ddot{x}_2, \cdots, \ddot{x}_n]^{\mathrm{T}}$ are the displacement, velocity and acceleration vectors, respectively. The letter (n) denotes the size of square matrices for n number of storey and T stands for transverse.

2.3 Natural period characteristics

A simple equation is derived that let us estimate the natural period of the n storey ordinary structure of Fig.2, a MDOF system, by using inter-storey parameters of the same structure which can be assumed as SDOF system. Note that the letters with overhead bars of Eq. (3a) and (3b) such as, natural period $\overline{T}$, damping ratio $\overline{\zeta}$, and the natural frequency $\overline{\omega}$, are the parameters of inter-storey of system-O, Fig. 4, that can be calculated by means of basic equations of structural dynamics.

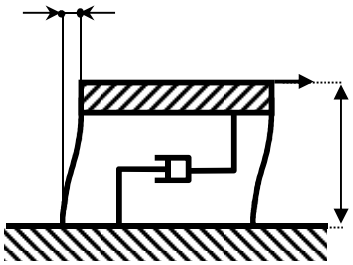

Fig. 4 Inter-storey section of system-O

$$\overline{T} = \frac{2\pi}{\overline{\omega}} \equiv 2\pi\sqrt{\frac{\overline{m}}{k}} \tag{3a}$$

$$\overline{\zeta} \equiv \frac{c}{2\sqrt{mk}} \tag{3b}$$

The eigenproblem of the undamped structure of system-O becomes as in Eq. (4a),

$$\left(K^{(n)}-\omega^2 M^{(n)}\right)\varphi^{(n)} = 0 \tag{4a}$$

Here, ω and $\varphi^{(n)}$ are the natural frequency and corresponding eigenvector. Eq. (4a) after substituting Eq. (4a) after substituting unit matrix I^(n) and the tri-diagonal stifness matrix Q^(n) becomes standard eigenvalue problem,

NOTE : I^(n) and Q^(n) should be same as in Eq. (4b) with superscript and italic,

$$\left(Q^{(n)}-\lambda^2 I^{(n)}\right)\varphi^{(n)} = 0 \tag{4b}$$

where λ is the eigenvalue. The natural frequency ratio λ_i, gives the ratio between the natural frequency of vibration model ω_i, and natural frequency of inter-story $\overline{\omega}$. Besides, the natural period of the vibration model T_i, and natural period of inter-story $\overline{T}$, becomes as follows,

$$\lambda_i = \frac{\omega_i}{\overline{\omega}} = \frac{\overline{T}}{T_i} \tag{5}$$

The eigenvector $\varphi_i^{(n)}$ is normalized to satisfy the orthogonal condition and δ_{ij} is treated as Kronecker delta, Eq. (6a) and Eq. (6b).

$$\varphi_i^{(n)\mathrm{T}} Q^{(n)} \varphi_j^{(n)} = \delta_{ij}\lambda_i^2 \tag{6a}$$

$$\varphi_i^{(n)\mathrm{T}} \varphi_j^{(n)} = \delta_{ij} \tag{6b}$$

Numerical equations of natural frequency ratio λ_i and eigenvector $\varphi_i^{(n)}$ become,

$$\lambda_i = 2sin\left(\frac{2i\text{-}1}{4n+2}\pi\right), \quad 1 \le i \le n \tag{7}$$

$$\varphi_i^{(n)} \equiv \left[\phi_{1,i}^{(n)}, \phi_{2,i}^{(n)}, \cdots, \phi_{n,i}^{(n)}\right]^{\mathrm{T}} \tag{8a}$$

$$\phi_{j,i}^{(n)} = \frac{2}{\sqrt{2n+1}} sin\left(\frac{2i\text{-}1}{2n+1} j\pi\right) \tag{8b}$$

After proportioning the Eq. (5) and Eq. (7), the ratio between the natural period of the vibration model and of inter-story can be estimated,

$$\frac{T_i}{\overline{T}} = \frac{1}{2} cosec\left(\frac{2i\text{-}1}{4n+2}\pi\right), \quad 1 \le i \le n \tag{9}$$

An approximate equation becomes as in follows of the first natural period on the basis of Eq. (9) in case that 1≪n,

$$T_1 \approx \frac{\bar{T}}{\pi}(2n+1) \tag{10a}$$

That is, the first natural period of structure can be extended as long as the number of storey n, increases for a specified natural period of inter-storey $\bar{T}$. The primary natural period for design use of the building can be calculated by following equation due to The Building Standard Law of Japan [13],

$$T_1 = \eta H \tag{10b}$$

where η, is specified respectively as 0.03 and 0.02 for Steel (S) and Reinforcement (RC) structures, The Building Standard Law of Japan [13]. Therefore, the first natural period is likely to be around 1 sec for mid-rise buildings of 40~60 m height. After proportioning the right sides of the Eq. (10a) and Eq. (10b), the approximate equation of inter-storey, for the first natural period, becomes,

$$\bar{T} \approx \frac{\pi\eta h}{2+1/n} \tag{11}$$

In section 6, these approximate equations' results will be compared to the results of numerical analyses using given parameters of illustrative example.

2.4 Viscous damping characteristics

The equation of viscous damping ratios of the vibration model and of inter-story becomes as in Eq. (12) by using the eigenvector of System-O, $\varphi_i^{(n)}$ and viscous damping ratio due to orthogonality condition of Eq. (8a) and Eq. (8b).

$$\frac{\zeta_i}{\bar{\zeta}} = \lambda_i = 2\sin\left(\frac{2i\text{-}1}{4n+2}\pi\right), \quad 1 \le i \le n \tag{12}$$

An approximate result can be obtained by derived Eq. (12) in case that, 1≪n for the first natural vibration vector,

$$\zeta_1 \approx \frac{\pi\bar{\zeta}}{2n+1} \tag{13a}$$

If the viscous damping ratio of the system-O is estimated for a specified $\bar{\zeta}$ the viscous damping ratio of the first mode is decreased as long as the number of storey, n increases. Considering, the viscous damping ratio of first mode of S and RC structures are around 1%~%5, and the relation between the structure height and the viscous damping ratio can be obtained after substituting the estimated viscous damping ratio ζ_1^*, into Eq. (13a).

$$\bar{\zeta} \approx \frac{2n+1}{\pi}\zeta_1^* \tag{13b}$$

3. FOLDED CANTILEVER SHEAR STRUCTURE

The main objective of the proposed building is to extend the first natural period almost two times by increasing the floor number by a factor of two in such a way that neither the number of storey n, nor structural height of ordinary structure H, has been altered. Therefore it is designed as an assembly of three different parts in one structure as seen in Fig. 5. The vibration model consists of a fix-supported shear sub-frame and movable shear sub-frame supported by roller bearings. These sub-frames are interconnected by a rigid connection frame at the top of the structure to enable separated sub-frames to move together as unique structure during any excitation.

In brief, it can be assumed that a $2n$-storey of ordinary structure with the height of $2H$ is equalized to n-storey of proposed structure with the height of H.

As mentioned in abstract, the numerical analyses were conducted on the idealized vibration model with and without additional viscous dampers. The vibration model given in Fig. 5, is named as system-AD since its additional dampers attached between the adjacent beams of fixed and movable sub-frames against excessive displacements.

Beams were named as B_1, B_2, ⋯, B_{i-1}, B_i, B_{i+1}, ⋯, B_{n-1} starting from the fixed shear sub-frame, Fig. 5. Then, the uppermost rigid connection beam was named as B_n. On the side of movable sub-frame, beams were continued to be named as B_{n+1}, B_{n+2}, ⋯, B_{j-1}, B_j, B_{j+1}, ⋯ and B_{2n}. Beam-$2n$ is the one that is supported by roller bearings and it can move along x and z directions.

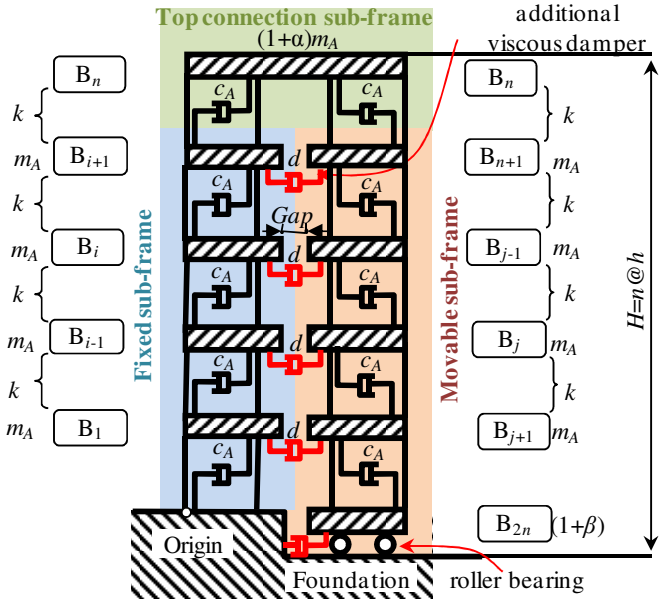

Fig. 5 Folded cantilever shear structure system-AD

The beams are carrying the concentrated masses of beam and columns at their center, and m_A represents the lumped masses of beams starting from beam-1 to beam-(n-1) on the side of fixed sub-frame, and from beam-(n+1) to beam-($2n$-1) on the side of movable sub-frame. The masses of beam-n and beam-$2n$ were represented as $(1+\alpha)m_A$ and $(1+\beta)m_A$ where α and β are the mass factors of B_n and B_{2n}, respectively. In the following sections, dynamic

parameters of the proposed vibration model were obtained for two different cases, $\alpha = \beta = 0$, that is, the mass of all beams are equal to each other, and $\alpha = 1$ and $\beta = 2$. Besides, each storey of idealized vibration model has equal structural damping ratio of dashpot c_A, and shear spring coefficient k_A.

In the section 4 and 5, the equations of motion for the proposed model without and with additional dampers are given, and dynamic parameters for two cases were obtained by numerical analyses.

4. FOLDED CANTILEVER SHEAR STRUCTURE WITHOUT ADDITIONAL DAMPERS

The proposed vibration model without additional dampers is illustrated in Fig. 6, and is named as system-A. System-A is identical to system-AD in every respect except additional dampers.

4.1 The equation of motion of undamped proposed structure under base excitation

The deformed frame and internal forces of system-A due to displacement excitation are illustrated in Fig. 6, under $z(t)$ time-varying ground motion, where z is the relative displacement of the base from its origin and $x_1, x_2, \cdots, x_{2n}$ are the lateral displacements of beam B_1, B_2, $\cdots$, B_{2n}.

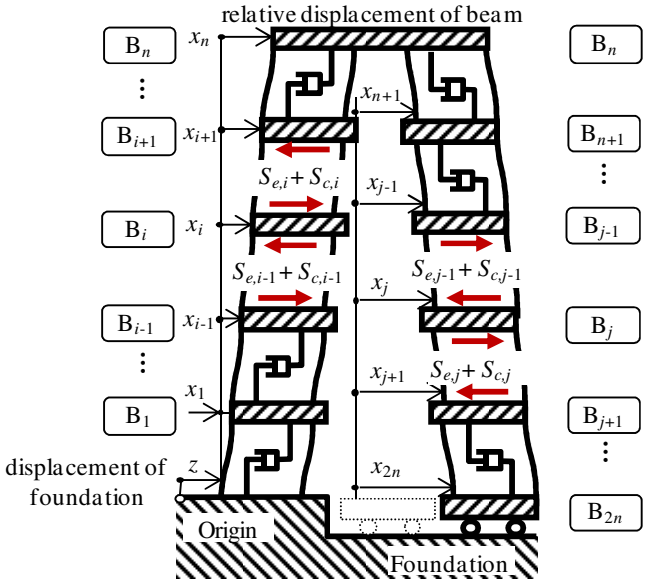

Fig. 6 Undamped folded cantilever shear structure system-A

The relative displacement of the i-th storey of the fixed sub-frame is $z + x_i$ with respect to origin, and shear and viscous damping forces between beam B_i and B_{i+1} are respectively, $S_{e,i}$ and $S_{c,i}$. On the opposite side, the shear and viscous damping forces between beam B_j and B_{j+1} are $S_{e,j}$ and $S_{c,j}$, respectively. The inertia forces of beams are $S_{m,1}$, $S_{m,2}$, $\cdots$, $S_{m,2n}$ for the beam B_1, B_2, $\cdots$, B_{2n}. The equilibriums of the forces on beams; B_i, B_j and B_n become,

$$-S_{m,i} + S_{c,i} - S_{c,i-1} + S_{e,i} - S_{e,i-1} = 0, \quad 1 \le i < 2n \tag{14a}$$

$$-S_{m,n} - S_{c,2n-1} - S_{e,2n-1} - f sgn(\dot{x}_{2n}) = 0 \tag{14b}$$

where, f is the coulomb frictional force resisting against the movement of beam B_{2n}. Besides, $S_{e,i} = k_A(x_{i+1}-x_i)$ and $S_{c,i} = c_A(\dot{x}_{i+1}-\dot{x}_i)$ are the shear and damping forces between the beams, respectively. As for beam B_{2n}, $S_{e,0} = k_A x_{2n}$, $S_{c,0} = c_A \dot{x}_{2n}$ and $S_{m,i} = m_A(\ddot{z}-\ddot{x}_{2n})$ are the shear, damping and inertia forces, respectively. After substituting these equations of the forces into Eq. (14a) and Eq. (14b), the equation of the motion of system-A becomes as the following equation,

$$M_A^{(2n)}\ddot{x}^{(2n)} + C_A^{(2n)}\dot{x}^{(2n)} + K_A^{(2n)}x^{(2n)} = -\ddot{z}M_A^{(2n)}p^{(2n)} - fe_{2n}^{(2n)}sgn(\dot{x}_{2n}^{(2n)}) \tag{15}$$

Here $e_i^{(2n)}$ is the $2n$ size of unit vector, and $\ddot{x}^{(2n)}$, $\dot{x}^{(2n)}$ and $x^{(2n)}$ are the acceleration, velocity and displacement matrix vectors that of $2n$ number of storey. $K_A^{(2n)}$, $C_A^{(2n)}$ and $M_A^{(2n)}$ are the stiffness, damping and mass matrices of Eq. (17).

$$K_A^{(2n)} = k_A Q^{(2n)} \tag{16a}$$

$$C_A^{(2n)} = c_A Q^{(2n)} \tag{16b}$$

$$M_A^{(2n)} = m_A(I^{(2n)} + J^{(2n)}) \tag{16c}$$

$$J^{(2n)} = \alpha e_n^{(2n)} e_n^{(2n)\mathrm{T}} + \beta e_{2n}^{(2n)} e_{2n}^{(2n)\mathrm{T}} \tag{16d}$$

Here $J^{(2n)}$is the mass matrix component of B_n and B_{2n} with α and β mass factors of different values, which is $2n$ size of square matrix in condition that all elements are equal to 0.

4.2 Natural period characteristics

Dynamic parameters of system-A can be obtained as in the following equations similar to system-O where $\bar{T}_A$, $\bar{\omega}_A$ and $\bar{\zeta}_A$ stands for natural period, circular frequency and damping ratio of inter-story, respectively.

$$\bar{T}_A = \frac{2\pi}{\bar{\omega}_A} = 2\pi\sqrt{\frac{m_A}{k_A}} \tag{17a}$$

$$\bar{\zeta}_c = \frac{c_A}{2\sqrt{m_A k_A}} \tag{17b}$$

If the coulomb frictional force of roller bearings is neglected, the eigenproblem becomes,

$$\{K_A^{(2n)} - \omega_A^2 M_A^{(2n)}\}\varphi_A^{(2n)} = 0 \tag{18a}$$

Here, ω_A and $\varphi_A^{(2n)}$ are the natural frequency and corresponding eigenvectors of undamped system. The Eq. (18a) after substituting Eq. (16a) and Eq. (16c) becomes,

$$\left\{Q^{(2n)}-\lambda_A^2\left(I^{(2n)}+J^{(2n)}\right)\right\}\varphi_A^{(2n)} = 0 \tag{18b}$$

where λ_A is the eigenvalue for System-A.

$$\lambda_{A,i}=\frac{\omega_{A,i}}{\bar{\omega}_A}=\frac{\bar{T}_A}{T_{A,i}} \tag{19}$$

Here $\lambda_{A,i}$ is the *i*-th natural frequency ratio and the corresponding eigenvector $\varphi_{A,i}^{(2n)}$ satisfies the orthogonality condition of following equations,

$$\varphi_{A,i}^{(2n)\mathrm{T}} Q^{(2n)} \varphi_{A,j}^{(2n)} = \delta_{ij}\lambda_{A,i}^2 \tag{20a}$$

$$\varphi_{A,i}^{(2n)\mathrm{T}}\left(I^{(2n)}+J^{(2n)}\right)\varphi_{A,j}^{(2n)} = \delta_{ij} \tag{20b}$$

In condition that the mass factors are equal to each other and zero, $\alpha = \beta = 0$, eigenvalues and eigenvectors of system-A can be calculated by using following equations after substituting $2n$ instead n of Eq. (7) and Eq. (8b),

$$\lambda_{A,i} = 2sin\left(\frac{2i\text{-}1}{4\times 2n+2}\pi\right) \tag{21}$$

$$\varphi_{A,i}^{(2n)} \equiv \left[\phi_{A,1,i}, \phi_{A,2,i}\ \cdots, \phi_{A,2n,i}\right]^{\mathrm{T}} \tag{22a}$$

$$\phi_{A,j,i} = \frac{2}{\sqrt{2\times 2n+1}} sin\left(\frac{2i\text{-}1}{2\times 2n+1} j\pi\right) \tag{22b}$$

By proportioning Eq. (19) and Eq. (21), the ratio between natural period of the vibration model, $T_{A,i}$ and of inter-story, $\bar{T}_A$ can be expressed as follows,

$$\frac{T_{A,i}}{\bar{T}_A} = \frac{1}{2} cosec\left(\frac{2i\text{-}1}{4\times 2n+2}\pi\right),\ 1 \le i \le n \tag{23}$$

An approximate equation becomes as follows to obtain the first natural period of system-A on the basis of Eq. (23), when $1 \ll n$,

$$T_{A,1} \approx \frac{\bar{T}_A}{\pi}(4n+1) \tag{24}$$

It can be estimated that the first natural period of vibration model is extended by increasing the number of storey n, for a given inter-story period $\bar{T}$, which can be calculated by means of specified mass and spring coefficient value, by comparing the Eq. (10a) and Eq. (24). The natural period of the system-A is almost two times than of system-O, Eq. (25) as long as the inter-story periods are same of system-A and system-O.

$$\frac{T_{A,1}}{T_1} \approx \frac{\bar{T}_A}{\bar{T}} \times \frac{4n+1}{2n+1} \approx 2\frac{\bar{T}_A}{\bar{T}} \tag{25}$$

4.3 Natural vibration mode characteristics

Fig. 7 presents the relation of system-O and system-A between the natural periods, the first, second and third natural periods, and the number of storey n, obtained by using Eq. (4b), Eq. (18b) and Eq. (23).

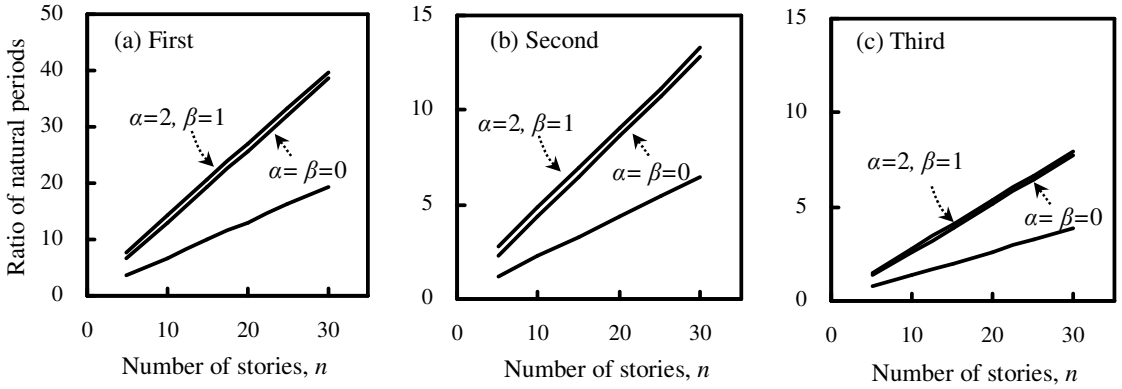

Fig. 7 The relation between natural period and storey number of undamped system-O and system-A

The relation of the natural period and number of storey of system-A was presented in two conditions; (i) $\alpha = \beta = 0$, that is, all masses are equal for each floor, and (ii) $\alpha = 2$, $\beta = 1$, that is, the mass of beam-n is three times and the mass of beam-2n two times of floor masses. The natural period of the former condition is calculated by using Eq. (23) and the latter condition by using eigenvalue λ_A obtained from the numerical solution of Eq. (18b) and regulated by Eq. (20). In Fig. 7, the natural period of the system-A is obtained around two times longer than of system-O. As for mass difference in condition that $\alpha = 2$, $\beta = 1$, the difference is quite small in terms of natural periods. As expected, natural periods are increased as long as the number of story increases.

Fig. 8 presents the first, second, third and fourth natural vibration modes of system-A obtained by using Eq. (22b) in condition that, $\alpha = \beta = 0$ and $n = 10$. To make it easy to understand, the floors of the fixed sub-frame are represented by black dots, ● whereas the movable sub-frame floors are represented by white dots, ○. The natural vibration mode shapes are plotted for each mode as shown in Fig. 8.

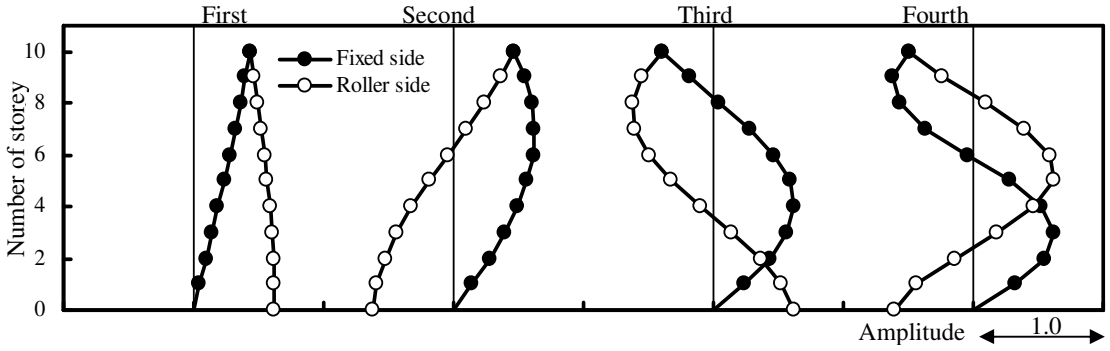

Fig. 8 Natural vibration modes of undamped system-A ($\alpha = \beta = 0$, n =10)

4.4 Viscous damping characteristics

The proportion of viscous damping ratios of the vibration model $\zeta_{c,i}$, and of inter-story $\bar{\zeta}_c$, becomes as in Eq. (26a) by using the eigenvector $\phi_{A,i}^{[2n]}$, and viscous damping ratio of system-A, due to orthogonality condition of Eq. (20a) and Eq. (20b) where the viscous damping ratio of inter-storey,

$$\frac{\zeta_{c,i}}{\bar{\zeta}_c} = \lambda_{A,\,i} \tag{26a}$$

Taking the mass factors as $\alpha = \beta = 0$, in Eq. (21), let us obtain the proportional damping ratios of $\zeta_{c,i}$ and $\bar{\zeta}_c$ as follows,

$$\frac{\zeta_{c,i}}{\bar{\zeta}_c} = \left(2sin \frac{2i-1}{4\times 2n+2} \pi \right) \tag{26b}$$

The approximate equation of the first natural damping constant can be estimated on the basis of the Eq. (26b) on condition that $1 << n$,

$$\zeta_{c,1} \approx \frac{\pi \bar{\zeta}_c}{4n+1} \tag{27}$$

It is seen that, the storey number n, and viscous damping constant $\zeta_{c,1}$ due to dashpots c_A have an inverse proportion as long as $\bar{\zeta}_c$ is specified. Proportioning the Eq. (13a) and Eq. (27) gives us the first viscous damping ratio equation of system-O and system-A.

$$\frac{\zeta_{c,1}}{\zeta_1} \approx \frac{\bar{\zeta}_c}{\bar{\zeta}} \times \frac{2n+1}{4n+1} \approx \frac{1}{2} \times \frac{\bar{\zeta}_c}{\bar{\zeta}} \tag{28}$$

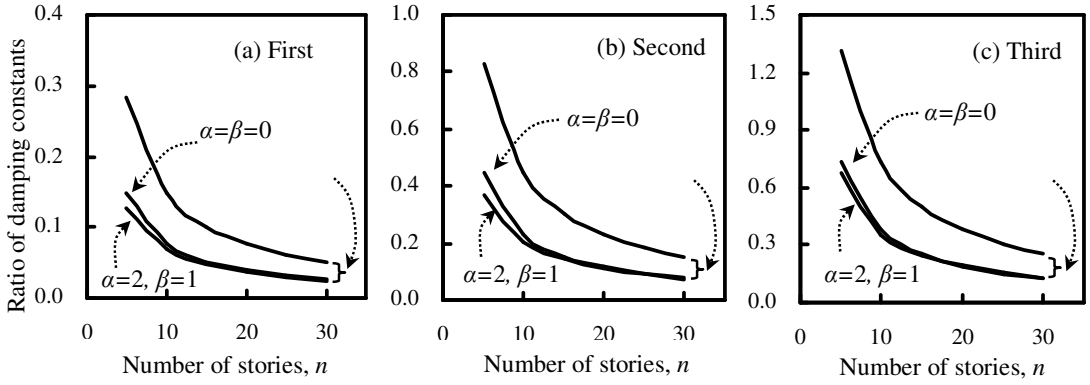

Fig. 9 Viscous damping constant – storey number relation between system-O and system-A

The viscous damping ratio of system-A becomes half of system-O for the same viscous damping ratio. Fig. 9 presents the relation between viscous damping ratio and number of storey n, for the first, second and third vibration modes, obtained by using Eq. (12) and Eq. (26b).

The mass factor conditions, α and β, of system-A is identical to conditions of Fig. 7. Damping ratio of system-A is obtained 1/2 of system-O for the same viscous damping constant value. Besides, the viscous damping constant of system-A, in condition that $\alpha = 2$, $\beta = 1$, differs a little in contrast in condition that $\alpha = \beta = 0$ for $n \leq 10$. But if the storey number increases, especially for $n \leq 10$, the difference becomes smaller.

5. FOLDED CANTILEVER SHEAR STRUCTURE WITH ADDITIONAL DAMPERS

As mentioned before, it is possible to increase natural period by increasing flexibility of the structure but this causes extreme displacements. Therefore, additional viscous dampers attached between the beams of sub-frames in the horizontal direction at each floor to reduce inter-story drifts and to increase damping ratio as well. System-A, is investigated again with supplemental dampers, and the new system called from hereafter as system-AD.

5.1 The equation of motion of damped proposed structure under base excitation

The deformed frame and internal forces of system-AD due to base excitation are illustrated in Fig. 10.

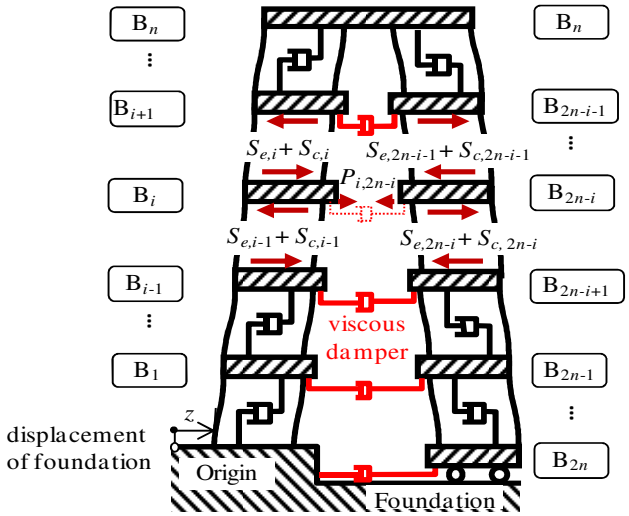

Fig. 10 Damped folded cantilever shear structure system-AD

The additional viscous damper opposing beam B_i and B_{2n-i} is removed and replaced by the $P_{i,2n-i}$ vectors of viscous damping force. The equilibriums of the forces for these opposite beams, B_i and B_{2n-i} become as follows,

$$-S_{m,i}+S_{c,i}-S_{c,i-1}+S_{e,i}-S_{e,i-1}+P_{i,j} = 0, \quad 1 \leq i < n \tag{29a}$$

$$-S_{m,j}+S_{c,j}-S_{c,j-1}+S_{e,j}-S_{e,j-1}-P_{i,j} = 0, \quad j = 2n-1$$

and the equilibrium of the forces for beam B_n and B_{2n} becomes as follows,

$$-S_{m,n}+S_{c,n}-S_{c,n-1}+S_{e,n}-S_{e,n-1} = 0 \tag{29b}$$

$$-S_{m,2n}-S_{c,2n-1}-S_{e,2n-1}-P_{0,2n} = 0$$

where, the viscous damping forces are , $P_{i,2n-i} = d\left(\dot{x}_{2n-1}-\dot{x}_i\right)$ and $P_{0,2n} = d(\dot{x}_{2n})$. By substituting these equations of the forces into the Eq. (29a) and Eq. (29b) the equation of the motion of system-AD becomes,

$$M_A^{(2n)}\ddot{x}^{(2n)}+\left(C_A^{(2n)}+D^{(2n)}\right)\dot{x}^{(2n)}+K_A^{(2n)}x^{(2n)} = -\ddot{z}M_A^{(2n)}p^{(2n)}-fe_{2n}^{(2n)}sgn\left(\dot{x}_{2n}^{(2n)}\right) \tag{30}$$

here, $D^{(2n)}$ is the damping matrix of the viscous damper d,

$$D^{(2n)} = dD_0^{(2n)} \tag{31a}$$

$$D_0^{(2n)} = e_{2n}^{(2n)}e_{2n}^{(2n)\mathrm{T}}+\sum_{i=1}^{n-1}\left[e_i^{(2n)},e_{2n-i}^{(2n)}\right]\begin{bmatrix}1 & -1\\ -1 & 1\end{bmatrix}\left[e_i^{(2n)},e_{2n-i}^{(2n)}\right]^{\mathrm{T}} \tag{31b}$$

5.2 Complex eigenvalue analysis

System-AD becomes non-proportional damping vibration system due to sequence characteristics of matrix $D_0^{(2n)}$ of Eq. (31b), and eigenvector $\varphi_{A,i}^{(2n)}$, cannot diagonalize the damping matrix $C_A^{(2n)}+D^{(2n)}$. Therefore, viscous damping ratio and complex eigenvalues of the non-proportional damping vibration system are obtained by using Foss Method [14]. If the coulomb friction force of roller bearings and damping matrix $C_A^{(2n)}$ of system-AD are neglected, the eigenproblem of the additional damped system becomes as follows,

$$\left\{\tau^2M_A^{(2n)}+\tau D_0^{(2n)}+K_A^{(2n)}\right\}\psi = 0 \tag{32a}$$

where τ and ψ are complex eigenfrequency and complex eigenvector of system-AD, respectively. When the $Q^{(2n)}$, $R^{(2n)}$and $D_0{}^{(2n)}$ matrices are substituted in Eq. (34a) the equation becomes,

$$\left\{\sigma^2\left(I^{(2n)}+J^{(2n)}\right)+2\sigma\bar{\zeta}_dD^{(2n)}+Q^{(2n)}\right\}\psi \tag{32b}$$

here, σ and $\bar{\zeta}_d$ are the complex eigenvalue and damping ratio, respectively.

$$\sigma = \frac{\tau}{\bar{\omega}_A} \tag{33}$$

$$\bar{\zeta}_d = \frac{d}{2\sqrt{m_Ak_A}} \tag{34}$$

Natural period $T_{d,i}$ and natural frequency $\omega_{d,i}$ of the *i*-th eigenvector of system-AD can be estimated as in follows,

$$\frac{T_{d,i}}{\bar{T}_A} = \frac{\bar{\omega}_A}{\omega_{d,i}} = \frac{1}{|\sigma_i|} \tag{35}$$

the natural period and the natural frequency equations due to Eq. (19) and Eq. (35) becomes as follows for the system-AD with additional dampers *d*,

$$\frac{T_{d,i}}{T_{A,i}} = \frac{\omega_{A,i}}{\omega_{d,i}} = \frac{\lambda_{A,i}}{|\sigma_i|} \tag{36}$$

and the viscous damping ratio $\zeta_{d,i}$ of the *i*-th eigenvector due to viscous damper supplementation can be calculated by the following formula,

$$\zeta_{d,i} = \frac{-Re(\sigma_i)}{|\sigma_i|} \tag{37}$$

Damping constant alterations of horizontally attached additional viscous dampers and vertically attached dashpots are illustrated in Fig. 11 obtained by Eq. (37) and Eq. (26b), respectively, in condition that $\alpha=\beta=0$. Viscous damping constants of dashpots, $\bar{\zeta}_c$ and additional viscous dampers, $\bar{\zeta}_d$ are specified as 0.3 and 0.01, respectively.

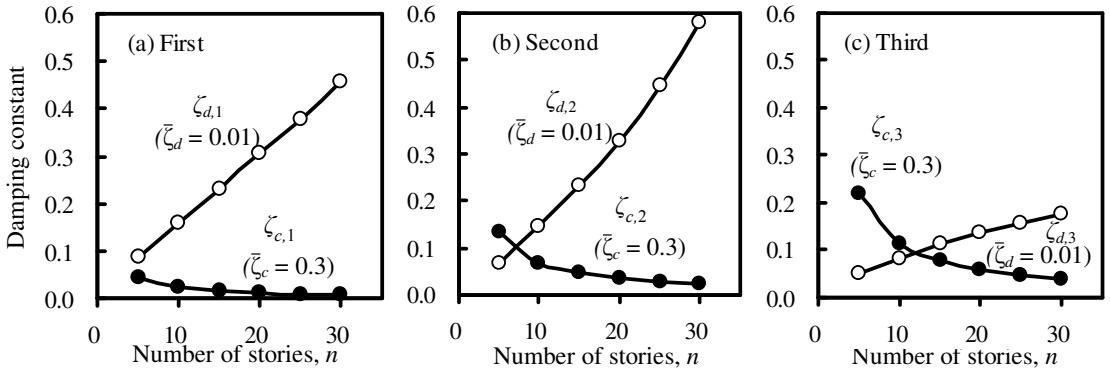

Fig. 11 Comparison of damping constant of additional viscous dampers and dashpots

By taking the first viscous damping constant of dashpot c_A as 0.02 for the n=10 storey structure, the viscous damping ratio of additional dampers become around 0.26 from Eq. (27). First natural vibration mode, Fig. 11a, shows that the damping constant of horizontal dampers is increased in proportion to number of storey *n*, whereas the damping constant of dashpots is decreased. In spite of similar damping constant for n=6 number of storey, the damping constant alteration becomes remarkable, up to 30 times, as long as the number of storey increases.

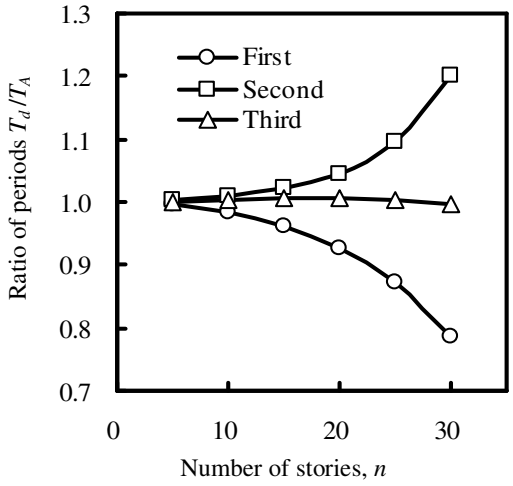

Fig. 12 Alteration of natural periods due to additional viscous dampers

Fig. 12 illustrates alteration of natural periods of first, second and third modes obtained using Eq. (36) due to additional viscous dampers. Calculation parameters are same with those of Fig. 11, except $\bar{\zeta}_c$ which was set to 0. The change was remained within 2% for the first mode of natural period and 1% for the second mode of natural period. The alteration for third mode of natural period was obtained very small. From Fig. 12, the horizontal placement of additional dampers was obtained more effective than of vertically attached dashpots. Besides, the natural period of first mode alteration was remained almost same due to additional dampers, Fig. 12. Therefore the proposed structure, system-AD, let us to extend the natural period of ordinary structure 2 times by increasing floor number and attaching additional dampers between opposing beams of sub-frames. Finally, the corresponding viscous damping ratio of the *i*-th natural frequency of system-AD can be obtained by substituting the damping matrix $C_A^{(2n)}$ of additional dampers into Eq. (32a), the viscous damping ratio of system-A,

$$\zeta_{AD,i} \approx \zeta_{A,i} + \zeta_{d,i} = \zeta_{c,i} + \zeta_{f,i} + \zeta_{d,i} \tag{38}$$

6. NUMERICAL ANALYSIS

To examine the theory of proposed structure, a set of numerical analyses including eigenvalue and elastic dynamic response analyses were performed through three idealized models, OCSS, system-O, and FCSS without and with additional dampers, system-A and system-AD, respectively. System-O is the comparison model for FCSS models. Besides, it is aimed to examine behavioral differences between FCSS without and with additional damper systems. Table 1 summarizes the structural model parameters of spring-mass models of numerical analyses. All models are 15-storey with 50 m of height (each storey height is 3.33 m).

Table 1. Spring-mass model parameters of numerical analyses.

Parameters	Folded cantilever shear structure(FCSS)	Ordinary cantilever shear structure(OCSS)
Total height, H	50 m	50 m
Number of stories, n	15	15
Story height, h	3.333 m	3.333 m
Story mass	m_1~m_{14}=50,000 kg m_{16}~m_{29}=50,000 kg m_{15}, m_{30}=100,000 kg	m_1~ m_{30}=100,000 kg
Total mass, m	1,600,000 kg	1,500,000 kg
Shear spring coefficient	k_1~k_{30}=1.60×10^8 N/m	k_1~k_{15}=3.85×10^8
Structural damping coefficient	c_1~c_{30}=1.11×10^6 Ns/m	c_1~c_{15}=2.50×10^6 Ns/m
First structural damping ratio	ζ_1=1.0 %	ζ_1=2.0 %
Additional damping coefficient	d_0~d_6=0.25×10^6 Ns/m	-
First additional damping ratio	$\Delta\zeta_1$=34.0 %	-
Frictional coefficient	μ=0.005	-
Frictional force (N)	f=41,650 N	-

The given parameters are not consistent and were specified due to a chart presenting the observed natural periods of Steel and Reinforcement concrete buildings of mid-rise buildings around Japan [15]. Natural period of 50 m building was assumed around 1 sec, then specifying mass of floor let us estimated shear spring coefficients for ordinary buildings.
For OCSS, columns are modeled as spring elements with 3.85x10^8 N/m of shear spring coefficient, which was represented as k_1, k_2, ···, k_{14} and k_{15}. The storey masses which were concentrated at the beams represented as m_1, m_2, ···, m_{14} and m_{15}, and each of them were equaled to 100.000 kg that makes the total mass 1.500.000 kg. Damping coefficients of the dashpots, c_1, c_2, ···, c_{14} and c_{15}, were set to 2.5x10^6 Ns/m.

FCSS models have the same height with OCSS model. The concentrated masses of the fixed shear sub-frame and movable shear sub-frames were represented as m_1, m_2, ··· m_{14}, and m_{16}, m_{17}, ···, m_{29}, m_{30}, respectively. The mass of each beam at the fixed and movable sides were, m_1~m_{14} and m_{16}~m_{30}, 50.000 kg. However the rigid connection beam, m_{15} was 100.000 kg. The total mass of the FCSS models became 1.550.000 kg. The shear spring coefficients, k_1~k_{15} and k_{16}~k_{30}, and the damping coefficients, c_1~c_{15} and c_{16}~c_{30}, were set to 1.60x10^8 N/m and 1.11x10^6 Ns/m, respectively. Structural damping ratio was also taken 1% for the system-A. System-AD is identical to system-A in terms of the structural height, structural damping ratio, masses, m_1~m_{30}, the spring coefficients, k_1~k_{30}, and the damping coefficients, c_1~c_{30}, except the additional viscous dampers with 0.25 x10^6 Ns/m damping coefficients represented as d_0~d_{14}.

6.1 Eigenvalue analysis

The natural frequencies, damping ratios and complex eigenvalues were given in Table 2 obtained by using Foss Method. The first natural period of the ordinary building was obtained $T_{1,O}$=0.99 sec, whereas the first natural periods of proposed building were obtained and $T_{1,AD}$=2.10 sec. According to the Eq. (11) and Eq. (25), natural periods were obtained, $T_{1,O}$=0.99 sec and $T_{1,AD}$=2.19 sec, respectively for the given parameters of Table 1. That is, proposed model acquired two times of first natural period compared to ordinary structure, and both results showed good match with each other. In addition, although the structural damping

coefficient of the system-A is taken smaller than OCSS, the damping ratio was obtained 9% for FCSS without damper and 35% for FCSS with damper, whereas OCSS has 2% of damping ratio. Besides, the damping ratio of system-A, which has no additional dampers, was obtained 9%.

Table 2. Frequencies and complex eigenvalues and damping ratios of the OCSS and FCSS with additional dampers.

	OCSS	FCSS with additional dampers		
	First	First	Second	Third
T_d (sec)	0.99	2.1	0.80	0.48
ω_d (rad/sec)	6.285	2.985	7.899	13.217
ζ	0.020	0.350	0.358	0.249
λ_R	-0.128	-1.046	-2.825	-3.285
λ_I	±6.284	±2.796	±7.377	±12.802

6.2 Elastic dynamic analysis

The elastic dynamic response analysis was conducted to investigate the seismic behavior of the numerical models due to El Centro (1940), Taft (1952), Hachinohe (1968) and Miyagi (1978) earthquakes. Fig. 14 illustrates El Centro earthquake seismic wave, and acceleration and displacement responses of system-O and AD.

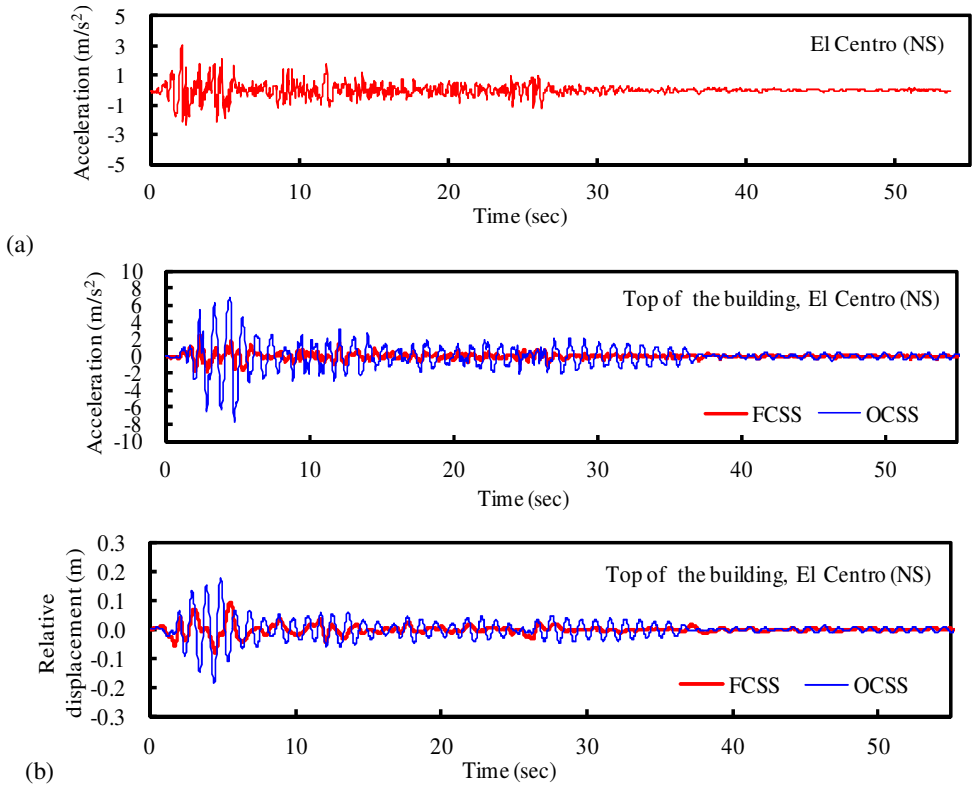

Fig. 13 El Centro earthquake, (a) seismic wave; (b) dynamic responses of FCSS with damper and OCSS.

The results shows that, the acceleration and displacement responses, with respect to base, of ordinary structure reduced up to 69% and 39%, respectively by proposed building. That is, structural responses can be mitigated properly by proposed structure compared to same height of ordinary building.

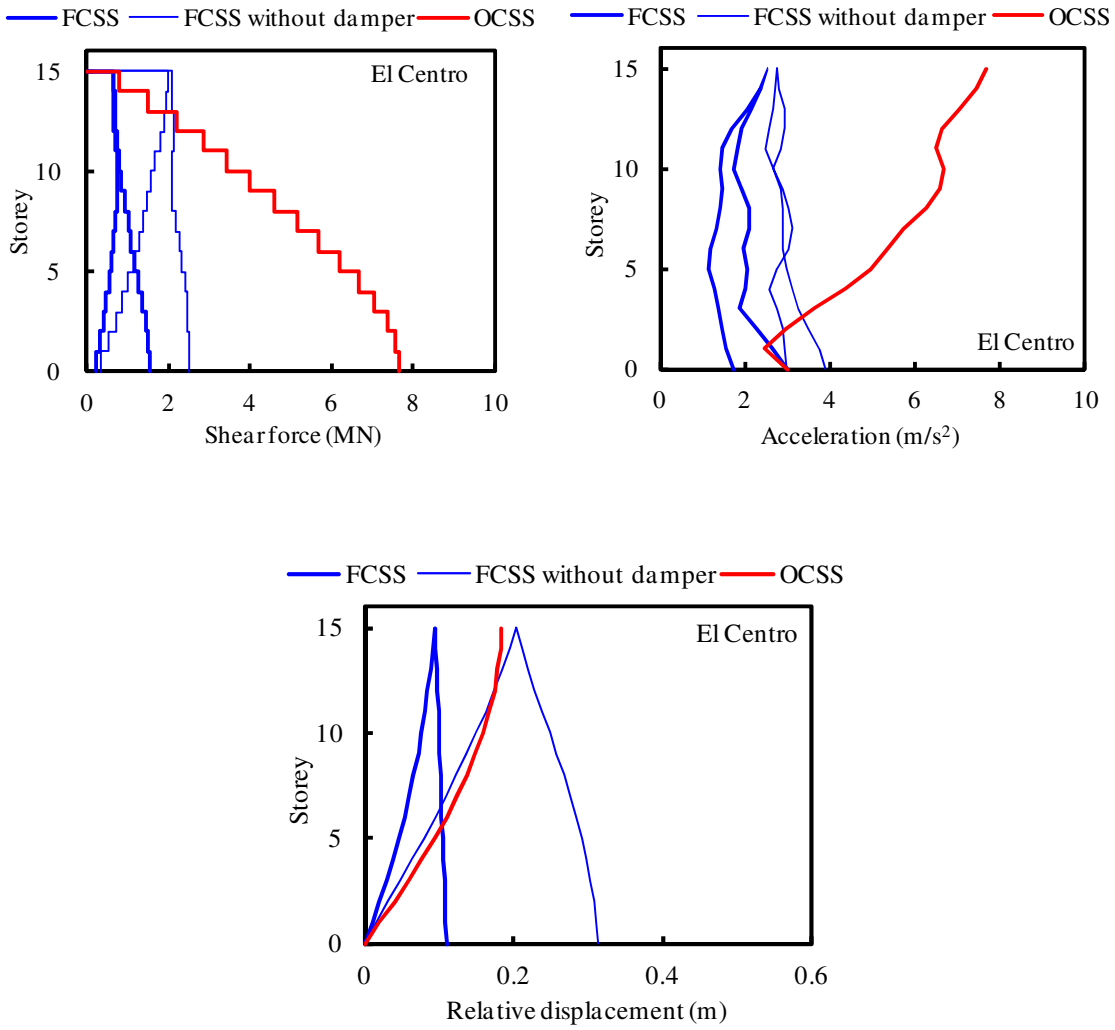

Fig. 14 Shear force responses of numerical vibration models due to seismic loads.

Shear force and acceleration responses were obtained maximum for ordinary building, then system-A and system-AD in decreasing response order, Fig. 14. Remarkably, displacements of system-A was relatively high. Therefore, it should be reduced by additional damper devices, and a further study about placement of these devices can be conducted on the base of methods which was mentioned in introduction section.

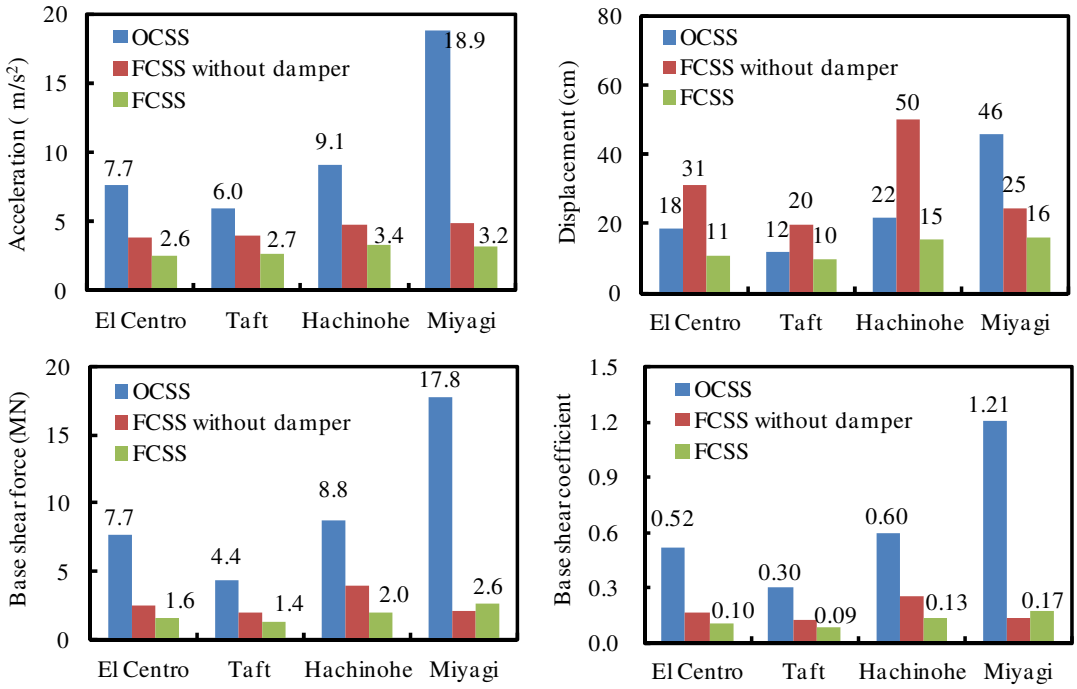

Fig. 15 Shear force responses of numerical vibration models due to earthquake waves.

Fig. 15 summarizes the building models responses under four earthquake waves. As expected, acceleration and base shear responses were highly reduced in case of proposed building. However, the displacement responses of proposed building without additional dampers with respect to base were higher compared to both ordinary building and proposed building with additional dampers.

7. CONCLUSION

In this paper, the newly designed folded cantilever shear structure was investigated theoretically and numerically with the aim of increasing the natural period and damping ratio to reduce seismic responses. For this purpose, a new seismic isolation approach was proposed incorporating base isolation system and coupling method into a mid-rise structure.
A new configuration for buildings of similar heights has been studied by connecting them at the roof part. The boundary conditions were selected to be one fixed supported building and the other one to be base isolated building while using rigid connection element at the top part. Based on the results, it is found that,

1. Coupling method was effective to incorporate base isolated and fixed supported frames in a building of similar heights by means of rigid connection sub-frame at the top part.
2. Proposed building is capable of extending the natural period two times compared to ordinary structure, which has the same number of storey, by increasing floor number two times without changing neither the total height of structure nor the number of storey.

3. The relative displacements with respect to the base of the proposed structure were relatively higher compared to ordinary building. Therefore, additional viscous dampers attached between sub-frames, and proposed structure with additional viscous dampers resulted in satisfying seismic performance.
4. These damping devices can be easily removed or added to the building between the sub-frames, and since these sub-frames can move toward each other or away from each other, it is an effective way placing damper devices in horizontal direction for increasing damping ratio.

REFERENCES

[1] Naeim F. and Kelly J.M. (1999), Design of Seismic Isolated Structures: From Theory to Practice, John Wiley & Sons Inc.
[2] Ohami K., Otani S. and Abe S. (2008), "Seismic Retrofit by Connecting to Adjacent Building", The 14th World Conference on Earthquake Engineering, Beijing, China.
[3] Ng C.L. and Xu Y.L. (2006), "Seismic response control of a building complex utilizing passive friction damper: experimental investigation", Earthquake Engineering and Structural Dynamics, 35, 657-677.
[4] Xu Y.L., He Q. and Ko J.M. (1999), "Dynamic response of damper-connected adjacent buildings under earthquake excitation", Engineering Structures, 21**,** 135-148.
[5] Aida T., Aso T., Takeshita K., Takiuchi T. and Fujii T. (2001), "Improvement of the structure damping performance by interconnection", Journal of Sound and Vibration, 242(2), 333-353.
[6] Agarwal V.K., Niedzwecki J.M. and van de Lindt J.W. (2007), "Earthquake induced pounding in friction varying base isolated buildings", Engineering Structures, 29, 2825-2832.
[7] Abdullah M.M, Hanif J.H, Richardson A. and Sobanjo J. (2001), "Use of a shared tuned mass damper (STMD) to reduce vibration and pounding in adjacent structures", Earthquake Engineering and Structural Dynamics, 30, 1185-1201.
[8] Lopez-Garcia D. (2001), "A simple method for the design of optimal damper configurations in MDOF structures", Earthquake Spectra, 17(3), 387-398.
[9] Luco J.E. and De Barros F.C.P (1998), "Optimal damping between two adjacent elastic structures", Earthquake Engineering and Structural Dynamics, 27, 649-659.
[10] Takewaki I. (2009), Building Control with Passive Dampers – Optimal Performance - based Design for Earthquakes, John-Wiley & Sons, London, UK
[11] Takewaki I. (1997), "Optimal damper placement for minimum transfer functions", Earthquake Engineering and Structural Dynamics, 26**,**1113-1124.
[12] Whittle J.K., Williams M.S., Karavasilis T.L. and Blakeborough A. (2012), "A Comparison of Viscous Damper Placement Methods for Improving Seismic Building Design", Journal of Earthquake Engineering, 16, 540-560.
[13] The Building Standard Law of Japan, Notification of MLIT, (2009), Notification No. 1793, 42.
[14] Foss K.A. (1958), "Co-ordinates which uncouple the equations of motion of damped linear dynamic systems", Journal of Applied Mechanics, (ASME), 32(3), 361-364.
[15] Damping in buildings (2000), Japanese Architectural Society. (In Japanese).